7-8-2009

Nanofiber Scaffolds with Gradations in Mineral Content for Mimicking the Tendon-to-Bone Insertion Site

Xiaoran Li

Jingwei Xie
Marshall University, xiej@marshall.edu

Justin Lipner

Xiaoyan Yuan

Stavros Thomopoulos

See next page for additional authors

Authors
Xiaoran Li, Jingwei Xie, Justin Lipner, Xiaoyan Yuan, Stavros Thomopoulos, and Younan Xia

NANO LETTERS

2009
Vol. 9, No. 7
2763-2768

Nanofiber Scaffolds with Gradations in Mineral Content for Mimicking the Tendon-to-Bone Insertion Site

Xiaoran Li,[†,‡] Jingwei Xie,[†] Justin Lipner,[†,§] Xiaoyan Yuan,[‡] Stavros Thomopoulos,[*,†,§] and Younan Xia[*,†]

Department of Biomedical Engineering, Washington University, St. Louis, Missouri 63130, School of Materials Science and Engineering, Tianjin Key Laboratory of Composite and Functional Materials, Tianjin University, Tianjin 300072, People's Republic of China, and Department of Orthopaedic Surgery, Washington University, St. Louis, Missouri 63110

Received May 19, 2009; Revised Manuscript Received June 9, 2009

ABSTRACT

We have demonstrated a simple and versatile method for generating a continuously graded, bonelike calcium phosphate coating on a nonwoven mat of electrospun nanofibers. A linear gradient in calcium phosphate content could be achieved across the surface of the nanofiber mat. The gradient had functional consequences with regard to stiffness and biological activity. Specifically, the gradient in mineral content resulted in a gradient in the stiffness of the scaffold and further influenced the activity of mouse preosteoblast MC3T3 cells. This new class of nanofiber-based scaffolds can potentially be employed for repairing the tendon-to-bone insertion site via a tissue engineering approach.

The attachment of dissimilar materials is a grand challenge because of the high levels of localized stress that develops at such an interface.[1] An effective biological solution to this problem can be found in the attachment of tendon (a compliant, structural "soft tissue") to bone (a stiff, structural "hard tissue").[2] The natural tendon-to-bone attachment relies on a gradient in structure and composition that translates into a spatial variation of mechanical stiffness.[2] Recent evidence supports the idea that this unusual spatial variation eliminates high levels of stress at the interface, providing effective transfer of mechanical load from tendon to bone. However, this unique transitional tissue between uninjured tendon and bone is not recreated during tendon-to-bone healing.[4] Surgical reattachment of these two dissimilar biological materials therefore often fails. For example, failure rates for rotator cuff repair (which requires tendon-to-bone healing) have been reported to be as high as 94%.[5] To address this clinical problem, it is critical to develop a new scaffold with a controllable gradation in mineral content along the surface. The gradation in mineral content can result in a spatial variation in the stiffness of the scaffold and thus be potentially used for repairing the tendon-to-bone insertion site via a tissue engineering approach.

Nanofibers can be routinely prepared as nonwoven mats by electrospinning from a wide variety of biocompatible and biodegradable polymers (both natural and synthetic), as well as composites containing inorganic materials.[6] Owing to the small feature size, a nonwoven mat derived from electrospun nanofibers typically exhibits a high porosity and large surface area and can thus mimic the hierarchical structure of extracellular matrix (ECM) critical to cell attachment and nutrient transport.[7] The fibers can also be conveniently functionalized by encapsulation or attachment of bioactive species such as ECM proteins, enzymes, nucleic acids, and growth factors to control the differentiation and proliferation of seeded cells.[7] Additionally, the nanofibers can be readily assembled into a range of arrays or hierarchically structured films by manipulating their alignment, stacking, and/or folding.[8] All these attributes make electrospun nanofibers well-suited as scaffolds for tissue engineering. In principle, the nanofiber-based scaffolds can be engineered with specific structural order, surface chemistry, degradation profile, biomechanical properties, and bioactivity for manipulating the attachment, proliferation, and differentiation of seeded cells and thus serve as a new framework for repairing or replacing the damaged tissue.[9]

Since the ECM of native bone is mainly composed of hydroxyapatite (HAp) dispersed in a framework of fibrous

* To whom correspondence should be addressed. E-mails: (Y.X.) xia@biomed.wustl.edu (for scaffold fabrication and cell culture study); (S.T.) ThomopoulosS@wudosis.wustl.edu (for mechanical property characterization).

† Department of Biomedical Engineering, Washington University.

‡ Tianjin University.

§ Department of Orthopaedic Surgery, Washington University.

10.1021/nl901582f CCC: $40.75
Published on Web 06/18/2009

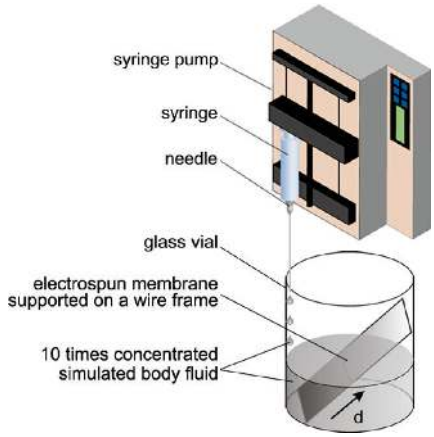

Figure 1. A schematic of the procedure for generating a graded coating of calcium phosphate on a nonwoven mat of electrospun nanofibers. Ten times concentrated simulated body fluid was added at a constant rate to linearly reduce the deposition time from the bottom to the top end of the substrate. The parameter *d* refers to the distance from the bottom edge of the substrate.

collagens, incorporation of calcium phosphate into electrospun nanofibers provides an effective route to the fabrication of scaffolds for bone tissue engineering. To this end, biomineralization, deposition of calcium phosphate from a simulated body fluid, is often used to generate the desired mineral coating on a nonwoven mat.[10] While this approach works well for bone, it will likely be ineffective at the interface between bone and soft tissues (e.g., bone-tendon, bone-cartilage, and bone-ligament), where gradients in structure (alignment of collagen fibers) and composition (mineral content) are required.[3] Such gradients are critical for the elimination of localized stress inherent in the attachment of dissimilar materials.[1] Two recent studies have started to address this issue. In the first study, Kalyon et al. developed a hybrid twin-screw extrusion/electrospinning technique for fabricating nonwoven mats of poly(ε-caprolactone) (PCL) fibers with a gradient of calcium phosphate formed between the top and bottom surfaces of the mat.[11] In the second study, Phillips et al. demonstrated that zonal organization of osteoblastic and fibroblastic cellular phenotypes can be engineered by seeding fibroblasts onto scaffolds containing a spatial distribution of retrovirus encoding the osteogenic transcription factor Runx2/Cbfa1.[12] The gradient of immobilized retrovirus was, in turn, achieved by controlling the densities of deposited poly(L-lysine). Such a gradient resulted in spatial patterns of transcription factor expression, osteoblastic differentiation, and mineralized matrix deposition. Here, we demonstrate a simple and versatile method that can be used to directly derivatize the surface of electrospun nanofibers with a gradient in calcium phosphate content. Further, we demonstrate that this gradient in mineral composition has functional consequences, leading to a spatial gradient in the stiffness of the scaffold and the activity of seeded cells.

Figure 1 shows a schematic of our approach for generating a graded coating of calcium phosphate on a nonwoven mat of electrospun nanofibers. Since the amount of mineral deposited from a solution is directly proportional to the immersion time, we can generate a gradient along the long axis of the substrate by varying the immersion time. In practice, this can be achieved by adding the mineral solution at a constant rate into a glass vial, which contains the substrate in a titled orientation. The concentration of the mineral solution, the titling angle of the substrate, and the feeding rate collectively determine the gradient profile. In the present study, we focused on two biocompatible and biodegradable polymers: poly(lactic-co-glycolic acid) (PLGA) and PCL. To improve the hydrophilicity of these two polymers and activate the surface for calcium phosphate deposition, we modified their surface by plasma treatment and/or gelatin coating.[13] For the mineral solution, we used 10 times concentrated simulated body fluid (10SBF), which contained concentrations of calcium and phosphate ions ten times higher than those found in human plasma or simulated body fluid (SBF). Inclusion of $NaHCO_3$ in the stock solution induced rapid deposition of calcium phosphate, enabling the formation of significant coating within a period of 2−6 h.[14] Our previous study revealed that incubation in 10SBF for 2 h could generate a relatively thick layer of calcium phosphate on a gelatin-coated electrospun PCL mats.[13] A similar phenomenon was also observed by Yang et al. for plasma-treated, electrospun PCL mats after immersion in 10SBF for 2 h.[15] The enhanced deposition of calcium phosphate in 10SBF makes our method feasible for generating a mineral gradient within a relatively short period of time. The variation in immersion time along the long axis of the substrate resulted in the formation of a continuous gradient in mineral content.

Figure 2 shows scanning electron microscopy (SEM) images taken from a plasma-treated PLGA sample at different locations along its long axis. Differences in morphology between these regions were apparent. At the bottom ($d = 0$), the fibers were covered by a thick layer of calcium phosphate (Figure 2a). Away from the bottom edge, the coating of calcium phosphate gradually became thinner. At $d \approx 6$ mm and $d \approx 9$ mm from the bottom, we observed the typical porous structure of a nonwoven mat (Figure 2b) and a nanotextured, flakelike mineral coating (Figure 2c), respectively. At the top end of the sample ($d \approx 11$ mm), there was essentially no mineral coating on the nanofibers (Figure 2d). To demonstrate the versatility of this approach, we have also applied it to nonwoven mats of gelatin-coated PCL nanofibers and essentially identical results were obtained (see Supporting Information, Figure S1).

In our previous study, we determined the crystal structure of the mineral phase deposited on the gelatin-coated PCL fibers by X-ray diffraction (XRD), and it was found that the mineral phase consisted of a mixture of HAp and dicalcium phosphate dehydrate (DCPD).[13] HAp has a composition close to that of mineral in bone and possesses excellent biocompatibility and bioactivity; DCPD, a possible precursor to HAp, is a potential raw material for bone substitute.[15] Clinically, many types of calcium phosphate have been employed in orthopedic surgery. For example, Mutsuzaki et al. prepared calcium phosphate-hybridized tendon by alternately soaking tendon in a Ca^{2+}-

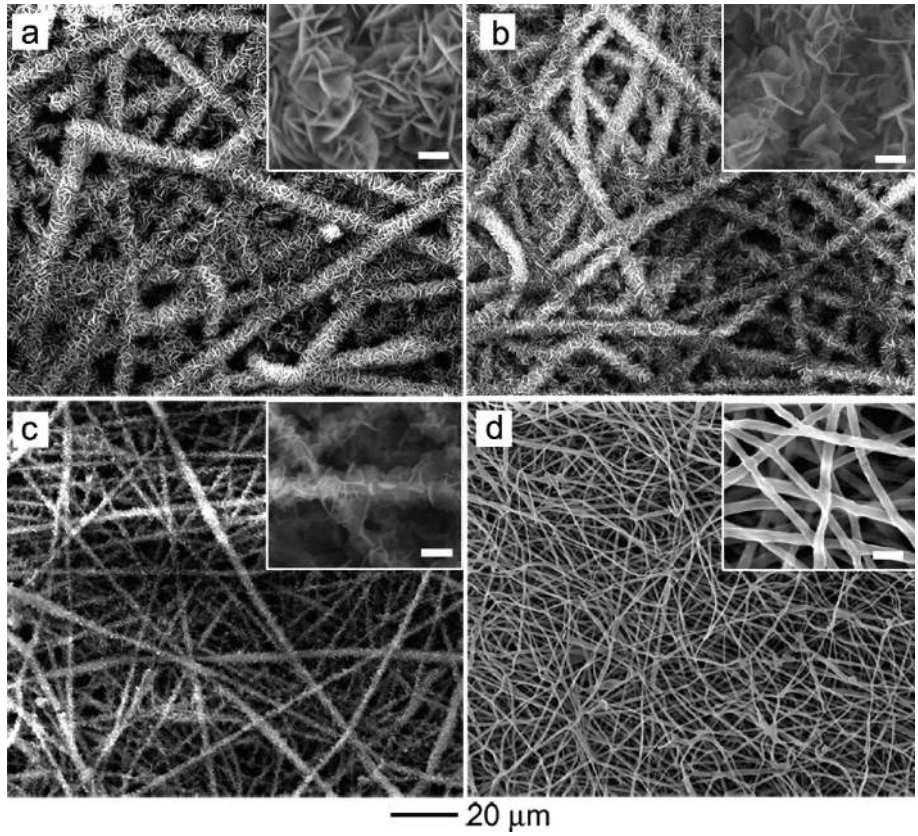

Figure 2. SEM images of calcium phosphate coatings on a plasma-treated nonwoven mat of PLGA nanofibers. The images were taken from different regions, with *d* corresponding to (a) 0, (b) 6, (c) 9, and (d) 11 mm. The scale bars in the insets are 2 μm.

containing solution and a PO_4^{3-}-containing solution.[16] They found that the calcium phosphate-incorporated tendon could enhance the healing process of anterior cruciate ligament (ACL) grafts at the tendon-to-bone interface and generated a direct insertion similar to the conventional ACL insertion within three weeks after implantation. In the present work, the mineral solution produced a calcium phosphate and polymer hybrid on the nonwoven mat of electrospun nanofibers with a continuous gradation in calcium phosphate content. The functionally graded constructs, especially with regard to mineral composition and mechanical property distributions, may significantly enhance tendon-to-bone healing.

To quantify the content of mineral in the graded calcium phosphate zone, we analyzed the atomic ratio of Ca/C at different locations using energy dispersive X-ray spectroscopy (EDX). Figure 3 shows the Ca/(Ca + C) ratio as a function of distance from the bottom edge of the scaffold for both the PLGA and PCL samples. As expected, the Ca/(Ca + C) ratios at different locations along the long axis of the substrate decreased linearly from 37.8 to 0.7% and from 33.9 to 0.8%, respectively, for the plasma-treated PLGA and gelatin-coated PCL fibers. We observed a linear correlation for both cases. We note that the distribution profile of the mineral content or gradient slope can be tailored to fit a specific application by controlling the feeding rate of mineral solution, the titling angle of the substrates, and/or the concentration of the mineral solution. We also found that presoaking the scaffold in 10SBF prior to the coating process could promote homogeneous nucleation and thus lead to the formation of a more significantly graded sample. Taken together, these results suggest that the current approach offers a simple and versatile method for generating gradations in mineral content on nanofiber scaffolds.

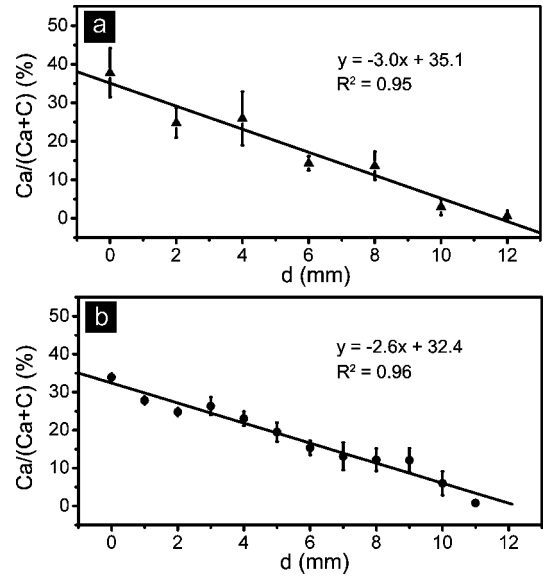

Figure 3. Characterization of the mineral content. The plots show average calcium content as a function of *d* along the direction of gradient for (a) plasma-treated PLGA scaffolds and (b) gelatin-coated PCL, respectively.

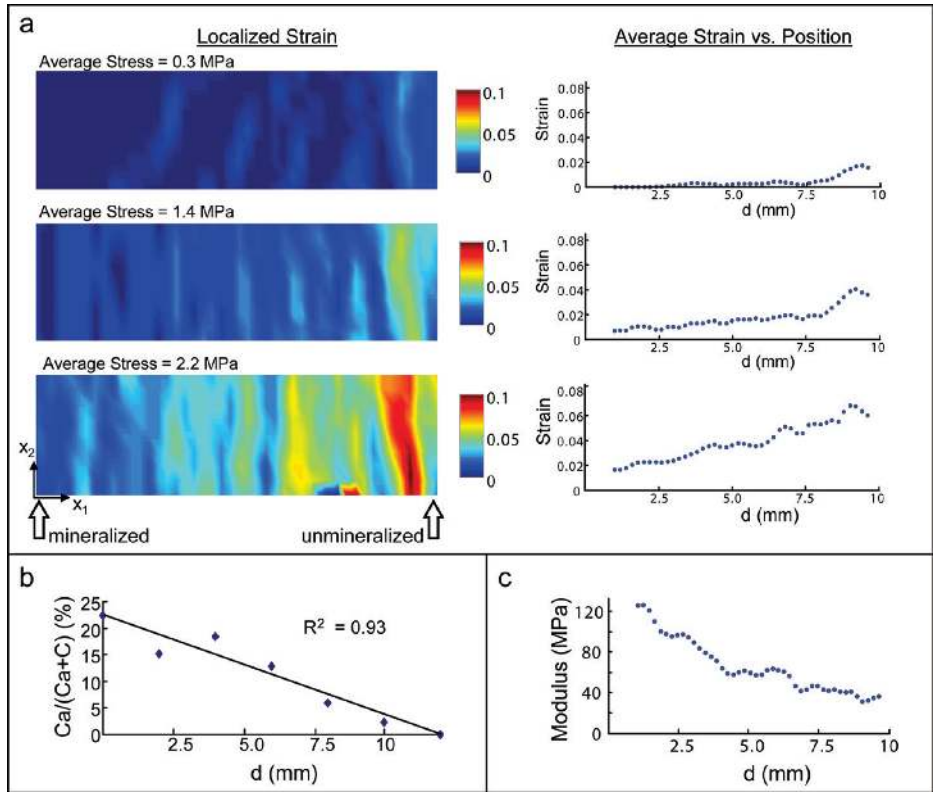

Figure 4. Mechanical testing of the graded scaffolds. There was a gradation in mechanical properties along the length of the scaffolds (a representative PLGA scaffold is shown). (a) The strains in the x_1 direction for three values of stress are shown. Localized strains are shown on the left and average strains are shown on the right. Strain increased with increasing stress and was highest on the unmineralized side of the scaffold. (b) There was a linear decrease in calcium phosphate along the length of the scaffold. (c) Young's modulus decreased with decreasing calcium phosphate content.

Figure 4 demonstrates that the gradient in mineral content had a functional consequence with regard to the mechanical properties of the scaffold. Under uniaxial tensile deformation, the local strain varied considerably along the long axis of the PLGA scaffold. Strain in the loading direction was lower at the mineralized end of the scaffold than the unmineralized end. Likewise, Young's modulus along the scaffolds increased with increasing levels of mineral, suggesting that the mineral coatings on the PLGA nanofibers observed by SEM had a stiffening effect on the nanofibers. Specifically, an increase of calcium content by 23% led to an approximately 2-fold increase in Young's modulus. This observed change in modulus due to changes in mineral content demonstrates the implementation of a "functional graded" material design, that is, designing a gradual variation in composition and structure over a distance to produce a change in the mechanical properties of the material.[17] This functionally graded material alleviates stress concentrations that would otherwise arise between two dissimilar materials (e.g., mineralized and unmineralized tissues).

Cell adhesion and migration assays can be used as simple and direct measures of biological function on gradated scaffolds. Cells in developing organs and tissues have the ability to detect and respond to various types of gradients by directed migration, a process called chemotaxis.[18] Previous studies indicated that graded patterns of biologic molecules were the driving force for migrating cells.[19] These gradients have been implicated in cell attachment.[20] Protein gradients may also play an important role in wound healing and for engineering blood vessels or nerves. Surfaces that were covalently modified with gradients of epidermal growth factor could induce directional cell migration and promote accelerated dermal wound healing.[21] Gradients of secreted signaling proteins could guide the growth of blood vessels during both normal and pathological angiogenesis.[22] Gradients of attractive and repulsive cues also play important roles during the development of complex neural network.[23] In the present work, we seeded mouse preosteoblast cells (MC3T3) onto a gelatin-coated PCL scaffold covered by a graded coating of calcium phosphate. MC3T3 cells have been extensively used to investigate adhesion, bone matrix formation, and the expression of bone related proteins.[24] It has been demonstrated that the addition of HA could enhance the attachment, spreading, and proliferation of MC3T3 cells.[25] Figure 5 shows a set of images taken at different locations along the long axis of the scaffold after three days of culture with MC3T3 cells. We note that the MC3T3 cells exhibited different adhesion behaviors and morphologies at different sites along the gradated scaffold. The region with the highest calcium phosphate content near the bottom edge of the substrate showed the highest level of cell density. Cells attached and spread very well. The regions with lower calcium phosphate content had significantly fewer adhered cells. Few cells were observed on the unmineralized end of the scaffold. We counted the cells at different regions. It is apparent that the cell density gradually decreased with

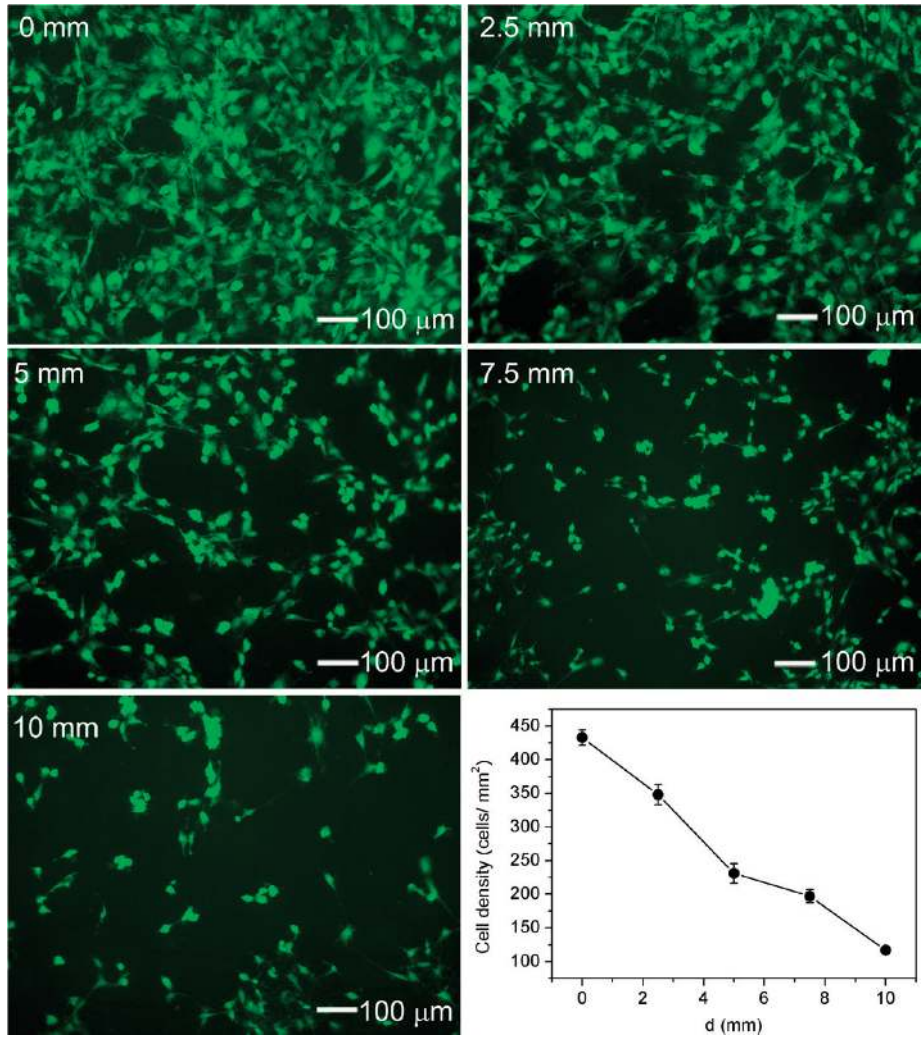

Figure 5. Cell culture data for the graded scaffolds. Fluorescence micrographs of MC3T3-E1 cells cultured on a graded scaffold made of gelatin-coated PCL nanofibers for 3 days and the average cell density as a function of *d* along the gradient. The images were taken from different regions (as indicated by *d*) along the gradient of calcium phosphate.

decreasing mineral content. These results showed that MC3T3 cells preferentially adhered to and/or proliferated in regions with higher calcium phosphate content along the gradated scaffold.

In summary, we have demonstrated a simple and versatile method that can be used to directly derivatize the surface of electrospun nanofibers with a gradient in calcium phosphate content. We further demonstrated that this gradient in mineral composition has functional consequences, leading to a spatial gradient in the stiffness of the scaffold and the activity of seeded cells. The approach demonstrated here might offer engineered scaffolds that can closely match the tendon-to-bone insertion site. In future studies, we will seek to combine these engineered scaffolds with mesenchymal stem cells to enhance tendon-to-bone healing in a rat rotator cuff injury and repair model.[4]

Acknowledgment. This work was supported in part by a Director's Pioneer Award from the NIH (DP1 OD000798-04) and startup funds from Washington University in St. Louis (to Y.X.), as well as a seed grant from the Center for Materials Innovation (CMI) at Washington University in St. Louis (to S.T.). X.L. is a visiting Ph.D. student from Tianjin University and was also partially supported by the China Scholarship Council.

Supporting Information Available: Detailed descriptions of experimental procedures and one additional figure are provided. This material is available free of charge via the Internet at http://pubs.acs.org.

References

(1) Barut, A.; Guven, I.; Madenci, E. *Int. J. Solids Struct.* **2001**, *38*, 9077.
(2) Thomopoulos, S.; Williams, G. R.; Gimbel, J. A.; Favata, M.; Soslowsky, L. J. *J. Orthop. Res.* **2003**, *21*, 413.
(3) (a) Zizak, I.; Roschger, P.; Paris, O.; Misof, B. M.; Berzlanovich, A.; Bernstorff, S.; Amenitsch, H.; Klaushofer, K.; Fratzl, P. *J. Struct. Biol.* **2003**, *144*, 208. (b) Katz, J. L.; Misra, A.; Spencer, P.; Wang, Y.; Bumrerraj, S.; Nomura, T.; Eppell, S. J.; Tabib-Azar, M. *Mater. Sci. Eng. C* **2007**, *27*, 450. (c) Wopenka, B.; Kent, A.; Pasteris, J. D.; Yoon, Y.; Thomopoulos, S. *Appl. Spectrosc.* **2008**, *62*, 1285.
(4) Thomopoulos, S.; Williams, G. R; Soslowsky, L. J. *J. Biomech. Eng.* **2003**, *125*, 106.
(5) Galatz, L. M.; Ball, C. M.; Teefey, S. A.; Middleton, W. D.; Yamaguchi, K. *J. Bone Joint Surg. Am.* **2004**, *86-A*, 219.
(6) Liao, S.; Li, B.; Ma, Z.; Wei, H.; Chan, C.; Ramakrishna, S. *Biomed. Mater.* **2006**, *1*, R45.
(7) Xie, J.; Li, X.; Xia, Y. *Macromol. Rapid Commun.* **2008**, *29*, 1775.

(8) Li, D.; Ouyang, G.; McCann, J. T.; Xia, Y. *Nano Lett.* **2005**, *5*, 913.
(9) Venugopal, J.; Low, S.; Choon, A. T.; Ramakrishna, S. *J. Biomed. Mater. Res., Part B* **2008**, *84B*, 34.
(10) Xu, A.; Ma, Y.; Colfen, H. *J. Mater. Chem.* **2007**, *17*, 415.
(11) Erisken, C.; Kalyon, D. M.; Wang, H. *Biomaterials* **2008**, *29*, 4065.
(12) Phillips, J. E.; Burns, K. L.; Doux, J. M. L.; Guldberg, R. E.; García, J. *Proc. Natl. Acad. Sci. U.S.A.* **2008**, *105*, 12170.
(13) Li, X.; Xie, J.; Yuan, X.; Xia, Y. *Langmuir* **2008**, *24*, 14145.
(14) Tas, A. C.; Bhaduri, S. B. *J. Mater. Res.* **2004**, *19*, 2742.
(15) Yang, F.; Wolke, J. G. C.; Jansen, J. A. *Chem. Eng. J.* **2008**, *137*, 154.
(16) Mutsuzaki, H.; Sakane, M.; Nakajima, H.; Ito, A.; Hattori, S.; Miyanaga, Y.; Ochiai, N.; Tanaka, J. *J. Biomed. Mater. Res.* **2004**, *70A*, 319.
(17) Birman, V.; Byrd, L. W. *Appl. Mech. Rev.* **2007**, *60*, 195.
(18) Wang, S.; Saadi, W.; Lin, F.; Nguyen, C. M.; Jeon, N. L. *Exp. Cell Res.* **2004**, *300*, 180.
(19) DeLong, S. A.; Moon, J. J.; West, J. L. *Biomaterials* **2005**, *26*, 3227.
(20) Mougin, K.; Ham, A. S.; Lawrence, M. B.; Fernandez, E. J.; Hillier, A. C. *Langmuir* **2005**, *21*, 4809.
(21) Stefonek, T. J.; Masters, K. S. *Wound Rep. Reg.* **2007**, *15*, 847.
(22) Barkefors, I.; Jan, S. L.; Jakobsson, L.; Hejll, E.; Carlson, C.; Johansson, H.; Jarvius, J.; Park, J. W.; Jeon, N. L.; Kreuger, J. *J. Biol. Chem.* **2008**, *283*, 13905.
(23) Kapur, T. A.; Shoichet, M. S. *J. Biomed. Mater. Res.* **2004**, *68A*, 235.
(24) Ku, Y.; Chung, C.; Jang, J. *Biomaterials* **2005**, *26*, 5153.
(25) Lee, K.; Wang, S.; Yaszemski, M. J.; Lu, L. *Biomaterials* **2008**, *29*, 2839.

NL901582F